Effect of the ATP-binding cassette drug transporters ABCB1, ABCG2, and ABCC2 on erlotinib hydrochloride (Tarceva) disposition in *in vitro* and *in vivo* pharmacokinetic studies employing Bcrp1$^{-/-}$/Mdr1a/1b$^{-/-}$ (triple-knockout) and wild-type mice

Serena Marchetti,[1] Nienke A. de Vries,[2] Tessa Buckle,[2] Maria J. Bolijn,[1] Maria A.J. van Eijndhoven,[1] Jos H. Beijnen,[1,3] Roberto Mazzanti,[4] Olaf van Tellingen,[2] and Jan H.M. Schellens[1,3]

Departments of [1]Experimental Therapy and Medical Oncology and [2]Clinical Chemistry, The Netherlands Cancer Institute, Amsterdam, The Netherlands; [3]Science Faculty, Department of Pharmaceutical Sciences, Division of Biomedical Analysis, Utrecht University, Utrecht, The Netherlands; and [4]Department of Internal Medicine, University of Florence, Azienda Universitario-Ospedaliera Careggi, Florence, Italy

Abstract

We tested whether erlotinib hydrochloride (Tarceva, OSI-774), an orally active epidermal growth factor receptor tyrosine kinase inhibitor, is a substrate for the ATP-binding cassette drug transporters P-glycoprotein (P-gp; MDR1, ABCB1), breast cancer resistance protein (BCRP; ABCG2), and multidrug resistance protein 2 (MRP2; ABCC2) *in vitro* and whether P-gp and BCRP affect the oral pharmacokinetics of erlotinib hydrochloride *in vivo*. *In vitro* cell survival, drug transport, accumulation, and efflux of erlotinib were done using Madin-Darby canine kidney II [MDCKII; wild-type (WT), MDR1, Bcrp1, and MRP2] and LLCPK (WT and MDR1) cells and monolayers as well as the IGROV1 and the derived human BCRP-overexpressing T8 cell lines. *In vivo*, the pharmacokinetics of erlotinib after p.o. and i.p. administration was studied in Bcrp1/Mdr1a/1b$^{-/-}$ (triple-knockout) and WT mice. *In vitro*, erlotinib was actively transported by P-gp and BCRP/Bcrp1. No active transport of erlotinib by MRP2 was observed. *In vivo*, systemic exposure (P = 0.01) as well as bioavailability of erlotinib after oral administration (5 mg/kg) were statistically significantly increased in Bcrp1/Mdr1a/1b$^{-/-}$ knockout mice (60.4%) compared with WT mice (40.0%; P = 0.02). Conclusion: Erlotinib is transported efficiently by P-gp and BCRP/Bcrp1 *in vitro*. *In vivo*, absence of P-gp and Bcrp1 significantly affected the oral bioavailability of erlotinib. Possible clinical consequences for drug-drug and drug-herb interactions in patients in the gut between P-gp/BCRP-inhibiting substrates and oral erlotinib need to be addressed. [Mol Cancer Ther 2008;7(8):2280–7]

Introduction

The ATP-binding cassette drug efflux transporters P-glycoprotein (P-gp; MDR1, ABCB1), breast cancer resistance protein (BCRP; ABCG2), and multidrug resistance protein 2 (MRP2; ABCC2) are involved in multidrug resistance, as they actively extrude a wide variety of anticancer drugs from tumor cells (1–3). Besides various tumor tissues, these transporters are expressed in several normal tissues (such as the intestine, liver, blood-brain barrier, and placenta syncythiotrophoblast), where they exert a protective role. They limit the intestinal uptake and the brain and fetal penetration of xenobiotics, and due to their localization in liver and kidney, they may facilitate the elimination of toxic compounds. Similarly, they can affect the pharmacologic behavior (absorption, distribution, metabolism, excretion, and toxicity) of various (anticancer) drug substrates (4).

Erlotinib hydrochloride (Tarceva, OSI-774, CP-358774) is a small-molecule, orally active, selective, and reversible epidermal growth factor receptor 1 tyrosine kinase inhibitor. Erlotinib, like its analogue gefitinib (Iressa, ZD1839), is a quinazoline derivative that competes with the binding of ATP to the intracellular tyrosine kinase domain of epidermal growth factor receptor, thereby inhibiting receptor autophosphorylation and blocking downstream signal transduction.

Several studies addressed the affinity of tyrosine kinase inhibitors, especially gefitinib, for the ATP-binding cassette drug transporters BCRP and P-gp (5). Gefitinib has been reported to inhibit BCRP and, to a lesser extent, P-gp function *in vitro* and *in vivo* (6, 7). Gefitinib was able to reverse resistance and enhance cytotoxicity of well-known BCRP/P-gp substrates, such as topotecan, mitoxantrone, irinotecan, and its active metabolite SN-38, in BCRP- or P-gp-overexpressing cells (8–12). Oral gefitinib has been reported to increase the oral bioavailability of irinotecan and topotecan (6, 13) and to enhance the central nervous system penetration of topotecan in mice (14). Other studies support the hypothesis that gefitinib is a substrate for BCRP

Received 11/1/07; revised 4/30/08; accepted 4/30/08.

The costs of publication of this article were defrayed in part by the payment of page charges. This article must therefore be hereby marked *advertisement* in accordance with 18 U.S.C. Section 1734 solely to indicate this fact.

Requests for reprints: Jan H.M. Schellens, Departments of Experimental Therapy and Medical Oncology, The Netherlands Cancer Institute, Plesmanlaan 121, 1066 CX Amsterdam, The Netherlands. Phone: 31-20-512-2446; Fax: 31-20-512-2572. E-mail: jhm@nki.nl

doi:10.1158/1535-7163.MCT-07-2250

(7, 15, 16) and a functional variant of ABCG2 (BCRP) has recently been associated with greater gefitinib accumulation in humans, thus supporting the hypothesis that BCRP expression and activity may affect the pharmacokinetics of gefitinib (16).

In contrast, studies evaluating the affinity of erlotinib for ATP-binding cassette drug efflux transporters are limited. A recent study indicates that erlotinib reverses ABCB1- and ABCG2-mediated multidrug resistance in cancer cells through direct inhibition of the drug efflux function of MDR1 and BCRP (16). The authors speculate also on a possible transport of erlotinib by MDR1 and BCRP, supported by the publication of Li et al., showing that erlotinib is a substrate of BCRP at relatively low concentrations and a BCRP inhibitor at high concentrations *in vitro* (17). However, the *in vivo* implications of these findings have not been explored yet. In addition, the affinity of erlotinib for MDR1 and MRP2 has not been reported.

Moreover, recently several drug-drug interactions involving erlotinib have been described and others are expected: treatment with erlotinib after administration of rifampicin resulted in 67% decrease in the area under the plasma concentration-time curve (AUC) for erlotinib in healthy volunteers (18). In another study, coadministration of erlotinib with ketoconazole significantly increased the systemic exposure to erlotinib (19–21). Considering that erlotinib is metabolized primarily by the CYP3A4 enzyme system (22) and that rifampicin and ketoconazole are well-known CYP3A4 inducer and inhibitor, respectively, these drug-drug interactions have been considered as primarily CYP3A4 mediated. However, given that rifampicin has been shown to induce also intestinal P-gp (23, 24) and that ketoconazole is a P-gp inhibitor (25, 26), although the effects of these two drugs on CYP3A expression/activity are expected to be greater and therefore more clinically relevant compared with the modulation of P-gp, a potential contribution of ATP-binding cassette drug efflux transporters to these interactions cannot completely be excluded.

Here, we investigated the affinity of erlotinib for P-gp, BCRP, and MRP2 using a panel of *in vitro* models, including the Madin-Darby canine kidney II epithelia cells (MDCKII) transfected with human MDR1 and MRP2 and mouse Bcrp1, the IGROV1 human ovarian cancer cell line and the T8 BCRP-expressing subline, and the porcine kidney epithelial cells (LLCPK) transfected with human MDR1. Moreover, we evaluated the effect of P-gp and BCRP on the p.o. and i.p. pharmacokinetics of erlotinib using Bcrp1/Mdr1a/1b$^{-/-}$ (triple-knockout) mice.

Materials and Methods

In vitro Studies

Chemicals and Reagents. Erlotinib hydrochloride and [^{14}C]erlotinib hydrochloride (129 μCi/mg) were kindly provided by Roche (Drs. J.W. Smit and Ch. Funk): in all *in vitro* and *in vivo* studies, the hydrochloride form of erlotinib was employed. For all *in vitro* studies, erlotinib hydrochloride was solved in DMSO (10 mg/mL). [^{3}H]insulin (0.78 Ci/mmol) was purchased from Amersham Biosciences. Pantoprazole (Pantozol 40 mg, Altana Pharma) was obtained from the pharmacy of The Netherlands Cancer Institute. Elacridar (GF120918) was a generous gift from GSK and zosuquidar trihydrochloride (LY335979) was kindly provided by Dr. P. Multani (Kanisa Pharmaceuticals). All other chemicals and reagents were from Sigma and of analytical grade or better.

Cell Lines. Polarized MDCKII cells, wild-type (WT) and stably expressing human MRP2 (ABCC2), human MDR1 (ABCB1), or mouse Bcrp1 (Abcg2), were kindly provided by Dr. A.H. Schinkel (The Netherlands Cancer Institute) and cultured as described previously (27–29).

The IGROV1 human ovarian adenocarcinoma and the IGROV1-derived resistant T8 cell lines were developed and cultured as described previously. T8 cells were exposed to 950 nmol/L topotecan weekly for 1 h, which keeps the resistance level in T8 constant for at least 25 weeks (30).

The polarized porcine kidney epithelial cell line (LLCPK) WT and MDR1, which were a generous gift from Dr. P. Borst (The Netherlands Cancer Institute), were employed as indicated previously (31).

All cell lines were grown at 37°C with 5% CO_2 under humidifying conditions.

Clonogenic Survival Assay. Exponentially growing MDCKII cells were trypsinized and plated (~100 per 3 mL medium/well for the MDCKII-WT, MDCKII-Bcrp1, and MDCKII-MRP2 cells; 150 per 3 mL medium/well for the MDCKII-MDR1 cells) in six-well microplates (~4 cm diameter/well; Costar) and allowed to attach for 8 h at 37°C under 5% CO_2. IGROV1 and T8 cells were plated (~200 per 4 mL medium/well) in 5-cm diameter dishes and incubated for 8 h for the cells to attach. After this attachment period, erlotinib hydrochloride was added at different concentrations. Cells were allowed to form colonies for 7 days (when MDCKII cells were used) or 14 days (when IGROV1 and T8 cells were used); subsequently, they were fixed and stained by 0.2% crystal violet/2.5 glutardialdehyde. The number of colonies containing at least 50 cells was visually counted under a light microscope. In each experiment, two replicates at each concentration of erlotinib were evaluated; at least three independent experiments with each cell line were done.

Transport across MDCKII and LLCPK Monolayers. Transport experiments were done in Costar Transwell plates with 3 μm pore membranes (Transwell 3414, Costar) as described previously (32). At least three independent experiments for each cell line and/or combination were done.

Accumulation and Efflux Experiments. Intracellular accumulation and efflux of erlotinib hydrochloride were measured in IGROV1 and T8 cells.

Cells were plated at a density of 1×10^6 in cell culturing plates (ø 4.8 cm, Costar) in 5 mL complete medium and allowed to grow to ~80% to 90% confluency.

In accumulation studies, plates were incubated for 30 min at 37°C with 5 mL complete medium containing 0, 5, 10, 15, 20, and 25 μmol/L erlotinib hydrochloride. After incubation, cells were washed twice with ice-cold PBS, scraped

immediately, collected in Falcon tubes, and centrifuged (2 min, 1,300 rpm, 0°C). Subsequently, the cells were resuspended in 1 mL of 0.1% acetic acid to lyse the cells. Protein concentrations were determined using the Bio-Rad assay based on the Bradford method (33). The concentration of erlotinib in the samples was determined by a validated high-performance liquid chromatographic analysis.

In efflux studies, IGROV1 and T8 cells were loaded with 15 μmol/L erlotinib hydrochloride for 30 min at 37°C. Subsequently, medium was removed and replaced by fresh medium. Immediately after the end of the incubation and at several following time points (1, 3, 6, 10, and 15 min), intracellular concentrations of erlotinib were measured with the same method employed in accumulation studies. Accumulation and efflux of erlotinib were determined in two replicates for each erlotinib concentration in at least three independent experiments.

In vivo Studies

Animals. Animals used were female WT and Bcrp1/Mdr1a/1b$^{-/-}$ (Bcrp1/P-gp knockout) mice [obtained by cross-breading Bcrp1$^{-/-}$ (34) and Mdr1a/1b$^{-/-}$ (35) mice], all with >99% FVB genetic background and between age 10 and 14 weeks. They were housed and handled according to institutional guidelines complying with Dutch legislation. Animals were kept in a temperature-controlled environment with a 12-h light/12-h dark cycle and received a standard diet (AM-II; Hope Farms) and acidified water *ad libitum*. To exclude a possible interaction with food in all experiments before the treatment of erlotinib mice were fasted for 4 h while kept in cages that would prevent coprofagy. All experiments involving animals were approved by the local animal ethics committee of our institute. At least 8 mice for each group were treated.

Drug Preparation and Administration. In *in vivo* studies, erlotinib hydrochloride was dissolved in DMSO and further diluted in acidified water (ratio 1:3) to obtain a final concentration of 0.25 mg/mL.

For pharmacokinetic studies, Bcrp1/Mdr1a/1b$^{-/-}$ and WT mice were treated p.o. or i.p. with 5 mg/kg erlotinib. The i.p. administration was chosen assuming good drug absorption and complete bioavailability. Sampling was done from the tip of the lateral tail vein in three series. During the first series, whole blood samples were collected at 15 min and 0.5, 1.5, 5, and 10 h after injection. Based on the results of this initial group, the sampling times of the two subsequent series were adapted to 5 and 15 min and 0.5, 1.5, 4, and 8 h after injection. After collection, the blood samples were immediately centrifuged and plasma was stored at -20°C until high-performance liquid chromatographic analysis took place.

High-Performance Liquid Chromatographic Analysis

Erlotinib hydrochloride was determined by reverse-phase high-performance liquid chromatography with UV detection at 330 nm. Separation was achieved using a Symmetry C18 column (150 × 2.1 mm, i.d.) and a mobile phase composed of 28% (v/v) methanol, 25% (v/v) acetonitrile, and 47% (v/v) 50 mmol/L potassium phosphate buffer containing 0.2% triethylamine (pH adjusted to 6.5 with hydrochloric acid). Sample pretreatment involved mixing of 200 μL plasma (standard, quality control, or unknown) with 50 μL internal standard (50 μg/mL midazolam in water) and 1 mL *tert*-butyl methyl ether for 5 min. After centrifugation (5 min, 5,000 × *g*), the aqueous layer was frozen on dry ice/ethanol and the organic top layer was decanted into a clean tube and dried by vacuum. Following reconstitution in 100 μL acetonitrile/water (20:80, v/v) by sonication/mixing, 50 μL were subjected to high-performance liquid chromatography. The calibration curve ranged from 20 to 1,000 ng/mL. Samples higher than 1,000 ng/mL were diluted with blank human plasma to fit into the dynamic range of the calibration curve. The lower limit of quantitation of the assay was 20 ng/mL when using 200 μL sample.

Pharmacokinetic and Statistical Analysis

Pharmacokinetic variables after administration of erlotinib hydrochloride were calculated using WinNonlin Professional (version 5.0, Pharsight). The AUC was calculated by employing the linear trapezoidal rule up to the last sampling point for each animal separately with extrapolation to infinity ($AUC_{0\text{-inf}}$) using the concentration at the last measured time point divided by the elimination rate constant k, which was obtained by log-linear regression analysis of data points of the elimination phase, by using WinNonlin. Data were accepted only if the contribution of the extrapolated area to the $AUC_{0\text{-inf}}$ was not greater than 20% of the total AUC.

Statistical analysis was done using Student's t test (two-tailed, unpaired). The bioavailability was calculated as the ratio of the AUC after p.o. and i.p. administration (assuming complete bioavailability after i.p. administration). The bioavailability of WT and Bcrp1/Mdr1a/1b$^{-/-}$ groups was compared after log transformation of the AUC data. Differences between two sets of data were considered statistically significant at $P < 0.05$.

Results

Cytotoxicity of Erlotinib

As expected due its noncytotoxic mechanism of action, the cytotoxicity of erlotinib hydrochloride in the cell lines tested employing the colony forming assay was low and in the micromolar range (Table 1). Moreover, visual inspection revealed differences in the dimension of the colonies of the applied cell lines and over the applied range of concentrations of the drug. At the same erlotinib concentration, the colonies were bigger in size in the MDR1- and BCRP/Bcrp1-expressing cells compared with WT cells, and in the same cell line, colonies were smaller (but still composed of at least 50 cells) at higher erlotinib concentrations. These results were interpreted as a sign that MDR1 and BCRP affect intracellular accumulation of erlotinib resulting in different growth characteristics in the colony forming assay.

Moreover, a small but statistically significant difference in IC_{50} was found between MDCKII-WT and MDCKII-MDR1 cells [resistance index (RI), 1.63; $P < 0.05$] and between WT and Bcrp1 cell lines (RI, 1.31; $P < 0.05$). A

Table 1. Cytotoxicity of erlotinib in IGROV1, T8, and MDCKII cell lines

	MDCKII-WT	MDCKII-Bcrp1		MDCKII-MDR1		MDCKII-MRP2		IGROV1	T8	
	IC_{50} (μmol/L)*	IC_{50} (μmol/L)*	RI†	IC_{50} (μmol/L)*	RI†	IC_{50} (μmol/L)*	RI†	IC_{50} (μmol/L)*	IC_{50} (μmol/L)*	RI†
Erlotinib	13 ± 0.6	17 ± 2.5	1.31‡	21.8 ± 0.9	1.63‡	12 ± 0.2	0.90	0.87 ± 0.2	1.82 ± 0.4	2.10‡

*Assessed by colony-forming assay after 7 d (in MDCKII cells) or 14 d (in IGROV1 and T8 cells) of drug exposure. Mean ± SD of at least three experiments.
†RI: ratio between the IC_{50} values of the resistant and parental cell lines.
‡Significant difference compared with its parental cells ($P < 0.05$).

significant difference in IC_{50} was also seen in the same assay employing IGROV1 and T8 cells (RI, 2.10; $P < 0.05$).

In contrast, no significant difference in IC_{50} of erlotinib was observed between MDCKII-WT and MDCKII-MRP2 cell lines ($P > 0.1$; Table 1).

These studies provided first hints that P-gp and BCRP mediate the transport of erlotinib and thereby affect cell survival. Based on these results, Transwell experiments were done at much lower and noncytotoxic concentrations of erlotinib.

Transport Experiments in MDCKII and LLCPK Monolayer Cells

Transport of Erlotinib by Bcrp1. Transport of erlotinib hydrochloride by Bcrp1 was studied using epithelial monolayers of MDCKII-Bcrp1 as well as WT cells as controls. Bcrp1 transported erlotinib (1.3 μmol/L) efficiently as can be seen by the >16-fold increased transport after 4 h from the basolateral to the apical side and decreased transport from the apical to the basolateral side in MDCKII-Bcrp1 (ratio of basolateral to the apical side to apical to the basolateral side: 17.09) compared with the WT monolayer (ratio of basolateral to the apical side to apical to the basolateral side: 1.03; Fig. 1). Furthermore, we showed that active transport of erlotinib was inhibited in MDCKII-Bcrp1 monolayer in the presence of the BCRP/P-gp inhibitors pantoprazole (500 μmol/L) or elacridar (5 μmol/L; Fig. 1).

Transport of Erlotinib by P-gp (MDR1). Active transport of erlotinib (1.3 μmol/L) was found in MDCKII-MDR1 and LLCPK-MDR1 monolayer cells. Indeed, transport of erlotinib was >3-fold increased in the MDCKII-MDR1 compared with the WT cell line (ratio of basolateral to the apical side to apical to the basolateral side after 4 h was 3.7 versus 1.2, respectively; data not shown). Similar results were obtained using LLCPK-MDR1 and WT monolayers (Fig. 2).

Furthermore, coincubation with the selective P-gp inhibitor zosuquidar (LY335979, 5 μmol/L; Fig. 2) or with pantoprazole (1.25 mmol/L; data not shown) resulted in complete inhibition of active transport of erlotinib by P-gp in MDCKII-MDR1 and LLCPK-MDR1 cell monolayers.

Transport of Erlotinib by MRP2. In contrast, no transport of erlotinib was found in Transwell experiments using MDCKII-MRP2 cell monolayers (data not shown).

Accumulation and Efflux of Erlotinib in IGROV1 and T8 Cells

To further investigate the role of BCRP in the transport of erlotinib, we did accumulation and efflux experiments in IGROV1 and T8 cells. Accumulation of erlotinib was ~1.4-fold lower in T8 compared with IGROV1 cells (data not shown).

In efflux experiments, a significantly increased initial efflux rate of erlotinib was found in the T8 cells compared with the IGROV1 cells: at 1 and 3 min after culturing in drug-free medium ~78% and 91.5% of intracellular erlotinib, respectively, effluxed from the T8 cells versus ~ 60% and 78%, respectively, from the IGROV1 cells (Fig. 3).

In vivo Pharmacokinetics of Erlotinib in Bcrp1$^{-/-}$/Mdr1a/1b$^{-/-}$ and WT Mice

To explore whether the observed transport of erlotinib by P-gp and BCRP/Bcrp1 *in vitro* is also relevant *in vivo*, we administered erlotinib p.o. and i.p. to WT and Bcrp1/Mdr1a/1b$^{-/-}$ mice.

At a dose of 5 mg/kg, there was a 1.49-fold statistically significant difference between $AUC_{0\text{-inf}}$ after p.o. administration of erlotinib comparing Bcrp1/Mdr1a/1b$^{-/-}$ and WT mice (7,419 ± 1,720 versus 4,957 ± 1,735 ng*h/mL respectively, $P = 0.01$; Table 2; Fig. 4). No significant difference in the AUC after i.p. administration of erlotinib was found between Bcrp1/Mdr1a/1b$^{-/-}$ and WT mice ($P > 0.2$; Fig. 4). The observed difference in the AUC between p.o. and i.p. administration was significant, which can at least partly be explained by incomplete absorption of erlotinib from the gastrointestinal tract.

The total plasma clearance of erlotinib, assuming complete bioavailability after i.p. administration, was not significantly different between WT and Bcrp1/Mdr1a/1b$^{-/-}$ mice (11.0 ± 1.8 and 11.1 ± 2.9 mg/L*h, respectively; $P > 0.1$).

The calculated apparent oral bioavailability was 60.4% (95% confidence interval, 48.6-75.0) and 40.0% (95% confidence interval, 27.8-57.7) for Bcrp1/Mdr1a/1b$^{-/-}$ and WT mice, respectively ($P = 0.02$, significantly increased in Bcrp1/Mdr1a/1b$^{-/-}$ mice; Table 2).

Discussion

Our *in vitro* data indicate that erlotinib hydrochloride is a substrate of P-gp and BCRP/Bcrp1 but not of MRP2. Also, data obtained *in vivo* support affinity for P-gp/Bcrp1, as the combined deletion of P-gp and Bcrp1 in the triple-knockout (Bcrp1/Mdr1a/1b$^{-/-}$) model resulted in a significantly increased systemic exposure and bioavailability after oral administration of erlotinib.

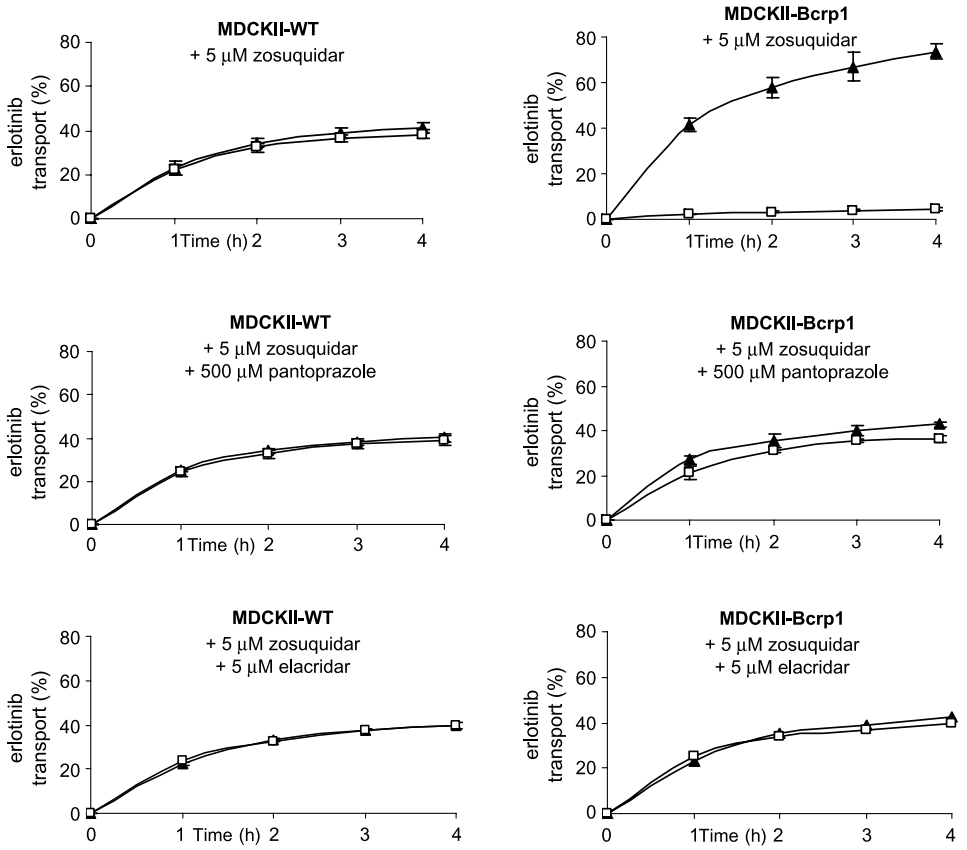

Figure 1. Transport of [^{14}C]erlotinib hydrochloride (1.3 μmol/L) across MDCKII-WT and MDCKII-Bcrp1 cell monolayers in the absence or presence of the BCRP/P-gp inhibitors pantoprazole (500 μmol/L) or elacridar (5 μmol/L). Labeled drug was added to either apical or basolateral compartment, and every hour up to 4 h, samples (200 μL) were obtained from both compartments. Appearance of radioactivity in the opposite compartment was measured and represented as the fraction (shown in percent) of total radioactivity added at the beginning of the experiment. Zosuquidar (LY335979, 5 μmol/L) was added to inhibit endogenous P-gp levels. [^{3}H]insulin leakage (to check the integrity of the monolayer) was tolerated up to 2% of the total radioactivity over 4 h. ▲, translocation from basal to apical compartment; □, translocation from apical to basolateral compartment. Mean ± SD of at least three experiments.

The first indication of affinity of erlotinib for P-gp and BCRP was obtained in *in vitro* studies employing cells overexpressing BCRP and P-gp. A small but statistically significant difference in IC_{50} was found between BCRP/Bcrp1- or P-gp-overexpressing and WT cell lines, which is apparently in contrast with the high rates of transport of erlotinib observed in Transwell experiments in Bcrp1- or P-gp-overexpressing cells. A first explanation for this discrepancy is that erlotinib is a growth factor inhibitor rather than a pure cytotoxic drug. This hypothesis is supported by the visual inspection of the plates obtained in the colony-forming assays, revealing a significant difference in growth characteristics of the colonies between cell lines and at applied different concentrations of the drug.

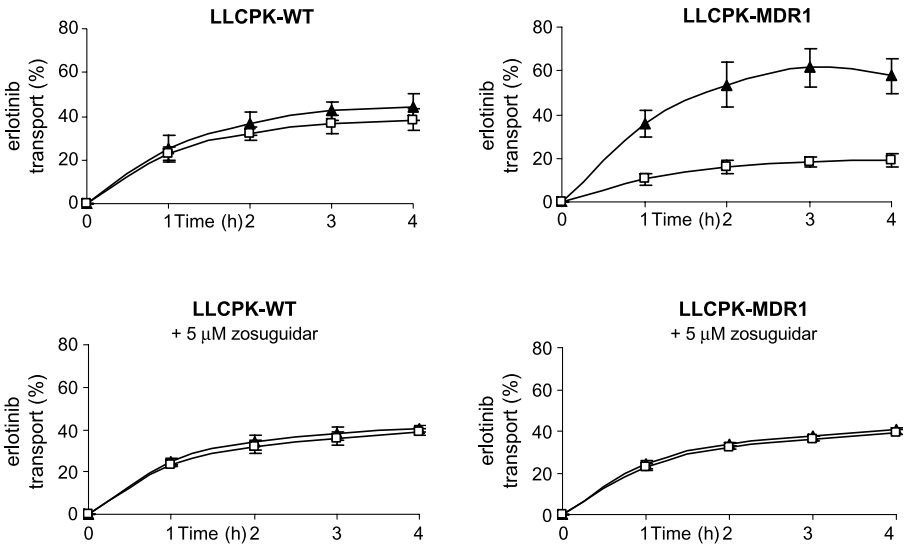

Figure 2. Transepithelial transport of [^{14}C]erlotinib hydrochloride (1.3 μmol/L) across LLCPK-WT and LLCPK-MDR1 cell monolayers in the absence or presence of the selective P-gp inhibitor zosuquidar (LY335979, 5 μmol/L). ▲, translocation from basal to apical compartment; □, translocation from apical to basolateral compartment. Mean ± SD of at least three experiments.

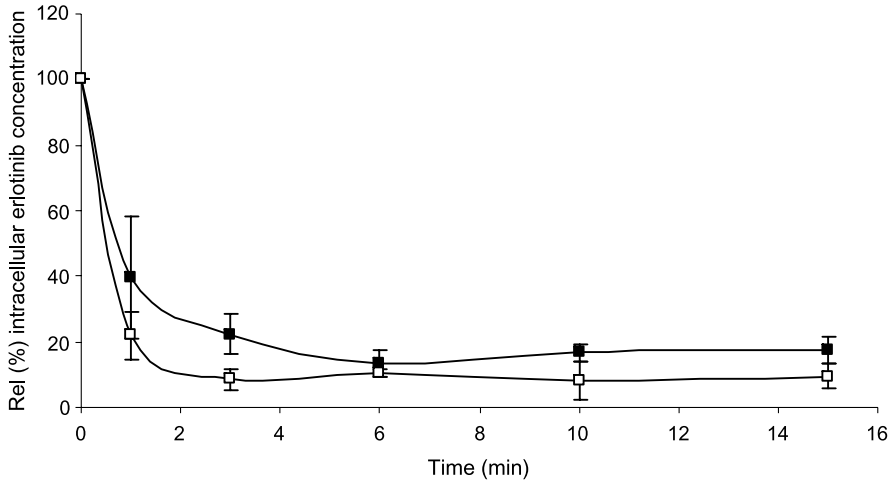

Figure 3. Efflux of erlotinib hydrochloride from IGROV1 (■) and T8 (□) cells. Cells were loaded for 30 min at 37°C with 15 μmol/L erlotinib hydrochloride. Subsequently, efflux of erlotinib from the cells was determined. *Points,* mean of three independent experiments; *bars,* SD.

At the same erlotinib concentration, the colonies were bigger in size in the MDR1- and BCRP-expressing cells compared with WT cells, and in the same cell line, colonies were smaller (but still composed of at least 50 cells) at higher erlotinib concentrations. Therefore, the difference in the IC_{50} value only may not be fully representative for the effect of MDR1 or BCRP overexpression on the cytotoxicity of erlotinib.

A second explanation may be that different concentrations of erlotinib were used in the different assays: in colony-forming and accumulation experiments, the concentrations of erlotinib used were significantly higher compared with Transwell experiments (between 25 and 5 μmol/L versus 1.3 μmol/L, respectively). It has recently been reported that erlotinib is transported by BCRP at lower concentrations, whereas at higher concentrations it is an effective BCRP inhibitor (16, 17). Therefore, it may be speculated that erlotinib at the higher concentrations used inhibited BCRP and/or P-gp activity, thus reducing its own efflux from the cells. This mechanism could potentially reduce the difference in resistance between WT- and BCRP/P-gp-overexpressing cells.

A third explanation could be that erlotinib, like other P-gp inhibitors, exerts a cytotoxic effect on P-gp-overexpressing cell lines at higher concentrations, interfering with the function of the plasma membrane.

Indeed, Transwell experiments clearly showed a significant active transport of erlotinib by Bcrp1 and MDR1 in MDCKII and LLCPK cell monolayers. LLCPK cells were used because MDCKII cells show a low level of endogenous P-gp expression. Transport of erlotinib from the basolateral to the apical side in Bcrp1-expressing monolayers was ~17-fold increased compared with the translocation of the drug from the apical to the basolateral compartment. Transport of erlotinib in MDCKII and LLCPK cell monolayers expressing MDR1 was >3-fold higher than in parental cells. Further evidence for the active transport of erlotinib by Bcrp1 and MDR1 was obtained in Transwell experiments done by coincubation with elacridar or pantoprazole (BCRP and P-gp inhibitors) or zosuquidar (a selective P-gp blocker), respectively, which completely inhibited the transport of erlotinib. In contrast, no difference in cytotoxicity was observed between MDCKII-WT and MDCKII-MRP2 cells and no active transport of erlotinib was found in MDCKII-MRP2 monolayers. These results suggest that erlotinib is not a substrate for MRP2.

To quantitate the effect of the absence of P-gp and Bcrp1 on the *in vivo* pharmacokinetics of erlotinib hydrochloride, we investigated the pharmacokinetics after p.o. and i.p. administration of the drug in WT and in Bcrp1/Mdr1a/$b^{-/-}$ mice. Results obtained after oral administration revealed that there is a statistically significantly increased AUC of erlotinib in triple-knockout compared with WT-mice (P = 0.01). In addition, the bioavailability of oral erlotinib was significantly increased in Bcrp1/

Table 2. Pharmacokinetic variables of erlotinib after p.o. and i.p. administration in WT and Bcrp1/Mdr1a/$1b^{-/-}$ mice

	WT	Bcrp1/Mdr1a/$1b^{-/-}$	P
AUC p.o. (ng*h/mL)*	4,957 ± 1,735	7,419 ± 1,720	0.01
AUC i.p. (ng*h/mL)†	11,873 ± 2,779	12,054 ± 1,896	>0.2 (NS)
Oral bioavailability (%; 95% confidence interval)	40.0 (27.8-57.7)	60.4 (48.6-75.1)	0.02

NOTE: Mean ± SE.
*AUC up to infinity after oral administration of erlotinib hydrochloride.
†AUC up to infinity after i.p. administration of erlotinib hydrochloride.

Mdr1a/b$^{-/-}$ mice, considering also the small and nonsignificant difference in the systemic clearance of erlotinib found between Bcrp1/Mdr1a/b$^{-/-}$ and WT mice. Therefore, effective inhibition of P-gp/BCRP in patients may significantly increase the systemic exposure to erlotinib, assuming that these results obtained in mice are representative for the clinical situation. This needs to be confirmed. Indeed, the increase in erlotinib exposure observed in triple-knockout mice may overestimate what would be observed in humans with functionally or genetically related impaired expression and/or activity of P-gp and BCRP. Moreover, although an effective inhibition of these transporters has been obtained in the clinic (36, 37), a complete block as well as a genetic absence of both transporters is unlikely in humans.

On the other hand, besides P-gp/BCRP, other transporters (in particular, uptake transporters in the gut) could be involved in erlotinib absorption, thus counteracting the activity of Bcrp1 and P-gp in the gut. This could explain the relatively high apparent oral bioavailability of erlotinib found in WT mice that have proficient Bcrp1 and P-gp. Furthermore, it cannot be excluded that as a consequence of P-gp and Bcrp1 gene deletion other transporters and/or drug-metabolizing enzymes involved in oral absorption of erlotinib are overexpressed in knockout mice, thus reducing the effect of Bcrp1/P-gp deletion on erlotinib pharmacokinetics. Indeed, considering that recently expression of CYP3A in the intestine has been shown to affect drug absorption (38) and that erlotinib has been reported to be susceptible to CYP3A-mediated metabolism (22, 39, 40), an altered expression/activity of CYP3A in our mice model might affect the magnitude of our findings. However, the bioavailability observed in WT mice is of the same magnitude as observed in humans (41) and the experimental condition in this model may thus reflect the pharmacokinetic condition in patients. It has been reported previously that food can significantly increase the bioavailability of erlotinib. In humans, the bioavailability increased from ~60% to ~90% when erlotinib was taken with food (42). For this reason, in our experiments, mice were fasted for 4 h before the treatment with erlotinib.

The biotransformation of erlotinib is complex and extensive. Besides incomplete uptake of erlotinib from the gut, extensive biotransformation during first-pass could contribute to the observed incomplete bioavailability. Furthermore, it can as yet not be excluded that other drug transporters are involved in the oral pharmacokinetics of erlotinib. Finally, in extrapolating results from animal models to humans, it is important to take into account that there are species differences in type and expression of transporters.

Conclusion

The experiments indicate that *in vitro* erlotinib is a substrate for P-gp as well as for BCRP/Bcrp1, whereas it does not seem to be transported by MRP2. In mice, a significantly increased systemic exposure and bioavailability after oral administration of erlotinib in Bcrp1/Mdr1a/1b$^{-/-}$ compared with WT mice was found. Complete inhibition of Bcrp1/Mdr1a/1b$^{-/-}$ resulted in an increase in the oral bioavailability of 66%.

In view of our results, potential implications of transporter pharmacogenetics on erlotinib pharmacokinetics variability and response (toxicity and efficacy) should be evaluated, because, as shown recently for another epidermal growth factor receptor tyrosine kinase inhibitor, gefitinib (17), functional variants of these ATP-binding cassette drug efflux transporters might be relevant to toxicity and antitumor activity of erlotinib. Moreover, possible clinical consequences of our results for drug-drug and herb-drug interactions at the intestinal level between oral erlotinib and P-gp/BCRP substrates and/or inhibitors warrant further investigation.

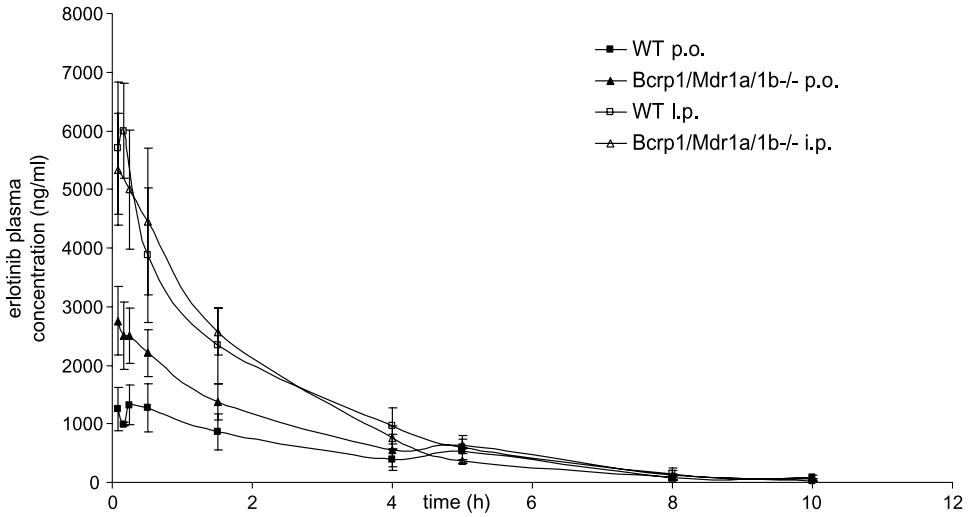

Figure 4. Plasma concentration time curves in WT (■, □) and Bcrp1/Mdr1a/1b$^{-/-}$ (▲, △) mice after p.o. and i.p. administration of erlotinib hydrochloride (5 mg/kg), respectively. At least 8 mice for each group were used. *Points,* mean concentrations for p.o. and i.p. administration; *bars,* SD.

Disclosure of Potential Conflicts of Interest

No potential conflicts of interest were disclosed.

Acknowledgments

We thank Drs. J.W. Smit and Ch. Funk for support, Dr. H. van Tinteren (statistician at The Netherlands Cancer Institute) for statistical analysis, and D. Pluim (Department of Experimental Therapy, The Netherlands Cancer Institute) for technical assistance.

References

1. Borst P, Elferink RO. Mammalian ABC transporters in health and disease. Annu Rev Biochem 2002;71:537 – 93.

2. Kruh GD, Belinsky MG. The MRP family of drug efflux pumps. Oncogene 2003;22:7537 – 52.

3. Schinkel AH, Jonker JW. Mammalian drug efflux transporters of the ATP binding cassette (ABC) family: an overview. Adv Drug Deliv Rev 2003;55:3 – 29.

4. Marchetti S, Beijnen JH, Mazzanti R, Schellens JHM. Clinical relevance: drug-drug interactions, pharmacokinetics, pharmacodynamics, and toxicity. In: You G, Morris ME, editors. Drug transporters: molecular characterization and role in drug disposition. Hoboken (NJ): Wiley-Interscience; 2007. p. 747 – 880.

5. Özvegy-Laczka C, Cserepes J, Elkind NB, Sarkadi B. Tyrosine kinase inhibitor resistance in cancer: role of ABC multidrug transporters. Drug Resist Updat 2005;8:15 – 26.

6. Leggas M, Panetta JC, Zhuang Y, et al. Gefitinib modulates the function of multiple ATP-binding cassette transporters *in vivo*. Cancer Res 2006;66:4802 – 07.

7. Özvegy-Laczka C, Hegedus T, Várady G, et al. High-affinity interaction of tyrosine kinase inhibitors with the ABCG2 multidrug transporter. Mol Pharmacol 2004;65:1485 – 95.

8. Kitazaki T, Oka M, Nakamura Y, et al. Gefitinib, an EGFR tyrosine kinase inhibitor, directly inhibits the function of P-glycoprotein in multidrug resistant cancer cells. Lung Cancer 2005;49:337 – 43.

9. Yanase K, Tsukahara S, Asada S, Ishikawa E, Imai Y, Sugimoto Y. Gefitinib reverses breast cancer resistance protein-mediated drug resistance. Mol Cancer Ther 2004;3:1119 – 25.

10. Nakamura Y, Oka M, Soda H, et al. Gefitinib (''Iressa,'' ZD1839), an epidermal growth factor receptor tyrosine kinase inhibitor, reverses breast cancer resistance protein/ABCG2-mediated drug resistance. Cancer Res 2005;65:1541 – 6.

11. Yang CH, Huang CJ, Yang CS, et al. Gefitinib reverses chemotherapy resistance in gefitinib-insensitive multidrug resistant cancer cells expressing ATP-binding cassette family protein. Cancer Res 2005;65:6943 – 9.

12. Nagashima S, Soda H, Oka M, et al. BCRP/ABCG2 levels account for the resistance to topoisomerase I inhibitors and reversal effects by gefitinib in non-small cell lung cancer. Cancer Chemother Pharmacol 2006;58:594 – 600.

13. Stewart CF, Leggas M, Schuetz JD, et al. Gefitinib enhances the antitumor activity and oral bioavailability of irinotecan in mice. Cancer Res 2004;64:7491 – 9.

14. Zhuang Y, Fraga CH, Hubbard KE, et al. Topotecan central nervous system penetration is altered by a tyrosine kinase inhibitor. Cancer Res 2006;66:11305 – 13.

15. Elkind NB, Szentpetery Z, Apati A, et al. Multidrug transporter ABCG2 prevents tumor cell death induced by the epidermal growth factor receptor inhibitor Iressa (ZD1839, gefitinib). Cancer Res 2005;65:1770 – 7.

16. Shi Z, Peng XX, Kim IW, et al. Erlotinib (Tarceva, OSI-774) antagonizes ATP-binding cassette subfamily B member 1 and ATP-binding cassette subfamily G member 2-mediated drug resistance. Cancer Res 2007;67:11012 – 20.

17. Li J, Cusatis G, Brahmer J, et al. Association of variant ABCG2 and the pharmacokinetics of epidermal growth factor receptor tyrosine kinase inhibitors in cancer patients. Cancer Biol Ther 2007;6:432 – 8.

18. Abbas R, Fettner S, Riek M. A drug-drug interaction study to evaluate the effect of rifampicin on the pharmacokinetics of the EGF receptor tyrosine kinase inhibitor, erlotinib in healthy subjects [abstract 548]. Proc Am Soc Clin Oncol 2003;22:137.

19. Hidalgo M, Bloedow D. Pharmacokinetics and pharmacodynamics: maximizing the clinical potential of erlotinib (Tarceva). Semin Oncol 2003; 30:25 – 33.

20. Birner A. Pharmacology of oral chemotherapy agents. Clin J Oncol Nurs 2003;7:11 – 9.

21. Kim TE, Murren JR. Erlotinib OSI/Roche/Genentech. Curr Opin Investig Drugs 2002;3:1385 – 95.

22. Ling J, Johnson KA, Miao Z, et al. Metabolism and excretion of erlotinib, a small molecule inhibitor of epidermal growth factor receptor tyrosine kinase, in healthy male volunteers. Drug Metab Dispos 2006;34:420 – 6.

23. Greiner B, Eichelbaum M, Fritz P, et al. The role of intestinal P-glycoprotein in the interaction of digoxin and rifampin. J Clin Invest 1999; 104:147 – 53.

24. Geick A, Eichelbaum M, Burk O. Nuclear receptor response elements mediate induction of intestinal MDR1 by rifampin. J Biol Chem 2001;276: 14581 – 7.

25. Iida N, Takara K, Ohmoto N, et al. Reversal effects of antifungal drugs on multidrug resistance in MDR1-overexpressing HeLa cells. Biol Pharm Bull 2001;24:1032 – 6.

26. Siegsmund MJ, Cardarelli C, Aksentijevich I, Sugimoto Y, Pastan I, Gottesman MM. Ketoconazole effectively reverses multidrug resistance in highly resistant KB cells. J Urol 1994;151:485 – 91.

27. Horio M, Chin KV, Currier SJ, et al. Transepithelial transport of drugs by the multidrug transporter in cultured Madin-Darby canine kidney cell epithelia. J Biol Chem 1989;264:14880 – 4.

28. Evers R, Kool M, van Deemter L, et al. Drug export activity of the human canalicular multispecific organic anion transporter in polarized kidney MDCK cells expressing cMOAT (MRP2) cDNA. J Clin Invest 1998;101:1310 – 9.

29. Pavek P, Merino G, Wagenaar E, et al. Human breast cancer resistance protein: interactions with steroid drugs, hormones, the dietary carcinogen 2-amino-1-methyl-6-phenylimidazol (4,5-*b*-)-pyridine, and transport of cimetidine. J Pharmacol Exp Ther 2005;312:144 – 52.

30. Maliepaard M, van Gastelen MA, de Jong LA, et al. Overexpression of the BCRP/MXR/ABCP gene in a topotecan-selected ovarian tumor cell line. Cancer Res 1999;59:4559 – 63.

31. Schinkel AH, Wagenaar E, van Deemter L, Mol CA, Borst P. Absence of the mdr1a P-glycoprotein in mice affects tissue distribution and pharmacokinetics of dexamethasone, digoxin, and cyclosporin A. J Clin Invest 1995;96:1698 – 705.

32. Breedveld P, Zelcer N, Pluim D, et al. Mechanism of the pharmacokinetic interaction between methotrexate and benzimidazoles: potential role for breast cancer resistance protein in clinical drug-drug interactions. Cancer Res 2004;64:5804 – 11.

33. Bradford MM. A rapid and sensitive method for the quantitation of microgram quantities of protein utilizing the principle of protein-dye binding. Anal Biochem 1976;72:248 – 54.

34. van Herwaarden AE, Jonker JW, Wagenaar E, et al. The breast cancer resistance protein (Bcrp1/Abcg2) restricts exposure to the dietary carcinogen 2-amino-1-methyl-6-phenylimidazo[4,5-*b*]pyridine. Cancer Res 2003;63:6447 – 52.

35. Schinkel AH, Smit JJ, van Tellingen O, et al. Disruption of the mouse mdr1a P-glycoprotein gene leads to a deficiency in the blood-brain barrier and to increased sensitivity to drugs. Cell 1994;77:491 – 502.

36. Kruijtzer CM, Beijnen JH, Rosing H, et al. Increased oral bioavailability of topotecan in combination with the breast cancer resistance protein and P-glycoprotein inhibitor GF120918. J Clin Oncol 2002;20:2943 – 50.

37. Malingré MM, Richel DJ, Beijnen JH, et al. Coadministration of cyclosporine strongly enhances the oral bioavailability of docetaxel. J Clin Oncol 2001;19:1160 – 6.

38. van Herwaarden AE, Wagenaar E, van der Kruijssen CM, et al. Knockout of cytochrome *P*450 3A yields new mouse models for understanding xenobiotic metabolism. J Clin Invest 2007;117:3583 – 92.

39. Li J, Zhao M, He P, et al. Differential metabolism of gefitinib and erlotinib by human cytochrome *P*450 enzymes. Clin Cancer Res 2007;13:3731 – 7.

40. Rakhit A, Pantze MP, Fettner S, et al. The effects of CYP3A4 inhibition on erlotinib pharmacokinetics: computer-based simulation (SimCYP) predicts *in vivo* metabolic inhibition. Eur J Clin Pharmacol 2008;64:31 – 41.

41. Frohna P, Lu J, Eppler S, et al. Evaluation of the absolute oral bioavailability and bioequivalence of erlotinib, an inhibitor of the epidermal growth factor receptor tyrosine kinase, in a randomized, crossover study in healthy subjects. J Clin Pharmacol 2006;46:282 – 90.

42. Johnson JR, Cohen M, Sridhara R, et al. Approval summary for erlotinib for treatment of patients with locally advanced or metastatic non-small cell lung cancer after failure of at least one prior chemotherapy regimen. Clin Cancer Res 2005;11:6414 – 21.

Molecular Cancer Therapeutics

Effect of the ATP-binding cassette drug transporters ABCB1, ABCG2, and ABCC2 on erlotinib hydrochloride (Tarceva) disposition in *in vitro* and *in vivo* pharmacokinetic studies employing Bcrp1$^{-/-}$/Mdr1a/1b$^{-/-}$ (triple-knockout) and wild-type mice

Serena Marchetti, Nienke A. de Vries, Tessa Buckle, et al.

Mol Cancer Ther 2008;7:2280-2287.